A solitary fibrous tumor arising in the parapharyngeal space, with MRI and FDG-PET findings

著者	Wakisaka Naohiro, Kondo Satoru, Murono Shigeyuki, Minato Hiroshi, Furukawa Mitsuru, Yoshizaki Tomokazu
journal or publication title	Auris Nasus Larynx
volume	36
number	3
page range	367-371
year	2009-06-01
URL	http://hdl.handle.net/2297/17608

doi: 10.1016/j.anl.2008.05.010

TITLE: “A Solitary Fibrous Tumor Arising in the Parapharyngeal Space, with MRI & FDG-PET Findings”

ABSTRACT

We present the imaging and pathological features of a 38-year-old man in whom a large parapharyngeal solitary fibrous tumor (SFT) on the left side was found. On MRI, the tumor showed a nodule-in-nodule appearance. The inner nodule revealed high signal intensities both on T1- and T2-weighted MR images. The entire tumor showed heterogeneous enhancement on gadolinium-enhanced T1-weighted images. ^{18}F-fluorodeoxyglucose (FDG) positron emission tomography (PET) identified heterogeneous radiotracer uptake of FDG in the inner nodule of the tumor. Histologic examinations revealed an admixture of growth patterns, including a “patternless pattern” and “haemangiopericytoma-like pattern”. The tumor was positive for CD34.

Imaging features of SFT arising in the parapharyngeal space are discussed with a review of literatures. This is the first report of FDG-PET finding of SFT arising in the head and neck. More cases are needed to achieve diagnostic significance from FDG-PET findings of parapharyngeal SFTs.

KEY WORDS

solitary fibrous tumor, parapharyngeal space, MRI, FDG-PET

INTRODUCTION

Solitary fibrous tumor (SFT) is a mesenchymal tumor that most frequently arises from the pleura [1]. Occasionally, SFTs arise in extrapleural sites such as the lung, mediastinum, pericardium, and meninges [1]. SFTs can also be found in various head and neck sites. Although rare, these locations have included the infratemporal fossa, parapharyngeal space, nose and paranasal sinuses, soft palate, epiglottis, as well as the thyroid, parotid, and submandibular gland [2-10]. Complete resection is the treatment of choice.

Herein, we report a case of SFT arising in the parapharyngeal space, describing the MRI, CT, and ^{18}F-fluorodeoxyglucose (FDG) positron emission tomography (PET) findings, with a review of the literatures.

CASE REPORT

A 38-year-old man presented with a persistent bulging mass on the left side of the oral cavity and gradually pronounced snoring. Physical examination revealed a large mucosally covered mass on the left side of the oropharynx. A mobile, painless, firm mass was also palpable in the left parotid region.

On contrast-enhanced CT images, the parapharyngeal tumor showed heterogeneous enhancement (Fig. 1A). The tumor was shown to have a nodule-in-nodule in appearance on MRI. On T1-weighted images, the outer nodule was isointense relative to muscle (Fig. 1B); however, the inner nodule demonstrated heterogenous signal varying from iso- to high-signal intensity. On T2-weighted images, the inner nodule demonstrated higher signal intensity centrally with a peripheral rim of mixed iso- to high-signal intensity (Fig. 1C). The tumor revealed heterogeneous enhancement on gadolinium-enhanced T1-weighted images except for the central part of the inner nodule (Fig. 1D). The corresponding PET scan identified heterogeneous uptake of FDG in the parapharyngeal tumor. The mass showed mild radiotracer uptake with some round foci of increased activity (Fig. 1E). A radiological diagnosis of a

mesenchymal tumor, specifically schwannoma involving the mandibular branch of the trigeminal nerve, was assumed and surgical treatment was planned. A transverse incision was made in the upper neck, and the mass was identified deep in the neck, on the lateral wall of the pharynx. The tumor was firm, measuring 65 x 50 x 40 mm, and the surface was macroscopically smooth and clearly identified. The tumor was not adhesive to the vessels or nerves, so it could be bluntly dissected from the surrounding tissue via a transcervical approach without mandibulotomy. The first bite syndrome was observed for several months after surgery, but it was spontaneously improved.

A yellowish-white nodule was shown in the fibrous nodule with a nodule-in-nodule growth pattern after cutting on gross examination (Fig. 2A). Histologic examination revealed that the tumor was mainly composed of spindle-shaped cells with varying amounts of collagen (Fig. 2B, D). The tumor cells and collagen tissue were arranged in a random pattern, known as a “patternless pattern” (Fig. 3A). There was moderate pleomorphism, occasional mitoses (1-2/10 high-power fields), and prominent vascularity with a “haemangiopericytoma-like pattern” (Fig. 3B). Immunohistochemically, the tumor tissue was strongly positive for CD34, a myeloid

progenitor cell antigen (Fig. 3C), but negative for S-100. On the basis of these findings, a final diagnosis of SFT, with a benign histologic appearance and areas of cellularity and degeneration was made (Fig. 2C).

DISCUSSION

SFT, an unusual type of spindle-cell lesion that is most often encountered in the pleura, can be quite difficult to diagnose because of its ability to simulate a variety of soft tissue neoplasms [11]. SFTs are characterized by a variety of growth patterns. The tumors commonly show narrow cords of cells with interspersed thick bundles of collagen (patternless pattern), admixed with areas showing a prominent haemangiopericytoma-like and angiofibroma-like appearance, neural-type fascicular areas with wavy nuclei, and occasional herring-bone formation. Most cases of solitary fibrous tumor are benign and cured with complete resection. Malignant SFTs are distinguished from benign SFTs only by an invasive growth pattern, high cellular pleomorphism, and abundant mitotic activity [1].

It has been reported that mature fibrous tissue usually has a lower signal intensity on T1- and T2- weighted images, and this is related to the area of hypocellularity and abundant collagen in the stroma [12, 13]. In the present case, the tumor showed a nodule-in-nodule appearance on MRI. The hypocellular, but more collagenous outer nodule in the tumor corresponded to the lower signal intensities both on T1- and

T2-weighted images compared with the hypercellular, but less collagenous inner nodule. Intense enhancement of SFTs is supposed to be due to its high vascularity. Lee et al. reported that the intratumoral low attenuation areas on T1-weighted images correlated with myxoid or cystic degeneration [14]. All these reports explain the compatibility of MRI findings with the histological findings of high vascularity and partial degeneration in the present case.

The imaging features of the nine previously reported SFTs of the parapharyngeal space are summarized in the Table. On MRI, all SFTs showed heterogenous high signal intensity on T2-weighted images. On contrast-enhanced T1-weighted images, heterogeneous enhancement was observed in four of five parapharyngeal SFTs and homogenous enhancement in one. On contrast-enhanced CT images, heterogeneous enhancement was observed in all SFTs arising in the parapharyngeal space. Thus, these findings are commonly observed in SFTs although they are not specific to this diagnosis. This is the first report of FDG-PET finding of SFT arising in the head and neck. Our FDG-PET findings identified hot areas in the inner nodule of the tumor, a hypercellular and less collagenous area. Although FDG-PET is typically helpful to differentiate

benign fibrous tumors from malignant mesotheliomas in pulmonary lesions [15], we need to collect more cases to achieve diagnostic significance from FDG-PET findings of head and neck SFTs.

REFERENCES

[1] England DM, Hochholtzer L, McCarthy MJ. Localized benign and malignant fibrous tumors of the pleura: a clinicopathological review of 223 cases. *Am. J. Surg. Pathol.* 1989;23:640-658.

[2] Kim HJ, Lee HK, Seo JJ, Kim HJ, Shin JH, Jeong AK, *et al*. MR imaging of solitary fibrous tumors in the head and neck. *Korean J. Radiol.* 2005;5:136-142.

[3] Hashimoto D, Inoue H, Ohbayashi C, Nibu K. Solitary fibrous tumor in the parapharyngeal space. *Otolaryngol. Head Neck Surg.* 2006;134:535-536.

[4] Cizmarevic B, Lanisnik B, Didanovic V, Kavalar R. Solitary fibrous tumor of the parapharyngeal space. *Wien. Klin. Wochenschr.* 2004;116:68-71.

[5] Jeong AK, Lee HK, Kim SY, Cho KJ. Solitary fibrous tumor of the parapharyngeal space: MR imaging findings. *Am. J. Neuroradiol.* 2002;23:473-475.

[6] Galera-Ruiz H, Martinez-Pozo A, Alos LL, Cardesa A, Traserra J. Single fibrous tumor of the parapharyngeal space. *Acta Otorrinolaringol.* 2000;51:457-459.

[7] Sato J, Asakura K, Yokoyama Y, Satoh M. Solitary fibrous tumor of the parotid gland extending to ther parapharyngeal space. *Eur. Arch. Otorhinolaryngol.*

1998;255:18-21.

[8] Gangopadhyay K, Taibah K, Manohar MB, Kfoury H. Solitary fibrous tumor of t he parapharyngeal space: A case report and review of the literature. *Ear Nose Throat J.* 1996;75:681-684.

[9] Al-Sinawi A, Johns AN. Parapharyngeal solitary fibrous tumour: an incidental finding at ENT examination. *J. Laryngol. Otol.* 1994;108:344-347.

[10] Safneck JR, Alguacil-Garcia A, Dort JC, Phillips SM. Solitary fibrous tumour: Report of two new locations in the upper respiratory tract. *J. Laryngol. Otol.* 1993;107:252-256.

[11] Moran CA, Suster S, Koss MN. The spectrum of histologic growth patterns in benign and malignant fibrous tumors of the pleura. *Sem. Diagn. Pathol.* 1992;9:169-180.

[12] Ferretti GR, Chiles C, Cox JE, Choplin RH, Coulomb M. Localized benign fibrous tumors of the pleura: MR appearance. *J. Comput. Assist. Tomogr.* 1997;21:115-120.

[13] Kransdorf MJ, Jelinek JS, Moser RP Jr, Utz JA, Hudson TM, Neal J, *et al*. Magnetic resonance appearance of fibromatosis. A report of 14 cases and review of the

literature. *Skeletal Radiol.* 1990;19:495-499.

[14] Lee KS, Im J-G, Choe KO, Kim CJ, Lee BH. CT findings in benign fibrous mesothelioma of the pleura: pathologic correlation in nine patients. *Am. J. Roentogenol.* 1992;158:983-986.

[15] Alexander M, Yang S, Yung R, Brasic JR, Pannu H. Diagnosis of benign solitary fibrous tumors by positron emission tomography. *South. Med. J.* 2004;97:1264-1267.

FIGURE LEGENDS

Fig. 1. (A) Contrast-enhanced CT findings. The tumor is located in the anterior compartment of the left parapharyngeal space. Heterogenous enhancement of the tumor was observed. The mass displaces the carotid sheath posterolaterally (large arrow), and parapharyngeal fat medially (arrow heads). The mandibular ramus was scalloped due to the large size of the tumor (small arrows). (B-D) MRI findings. The parapharyngeal tumor showed a nodule-in-nodule appearance. (B) Axial T1-weighted MRI. Inner nodule showed iso- to high- signal intensity. (C) Axial T2-weighted MRI. Inner nodule showed heterogenous high-signal intensity. Outer nodule revealed iso- to high-signal intensity. (D) Axial gadolinium-enhanced T1-weighted MRI demonstrated the strong enhancement of the tumor except for a part of the inner nodule. (E) Axial ^{18}F-fluorodeoxyglucose (FDG) positron emission tomography (PET) findings show heterogeneous increased uptake of FDG in the tumor in the left parapharyngeal space (arrow).

Fig. 2. (A) Gross examination of the tumor revealed a nodule-in-nodule growth pattern.

(B) Microscopic examination of the inner nodule showed a hypercellular, but less collagenous histology. A part of the inner nodule showed an area with degeneration (C). (D) The outer nodule presented a hypocellular, but more collagenous area, in contrast to the inner nodule.

Fig. 3. The admixture of two or more growth patterns within the same lesion is a characteristic histological feature of solitary fibrous tumor. (A) The tumor is composed of narrow cords of cells with interspersed thick bundles of collagen (patternless pattern). (B) Tumor cells are arranged around collapsed, irregular, branching capillaries and large vessels. (C) Immunohistochemical staining of the tumor with anti-CD34, a myeloid progenitor cell antigen, identified strong immunoreactivity in the tumor cells.

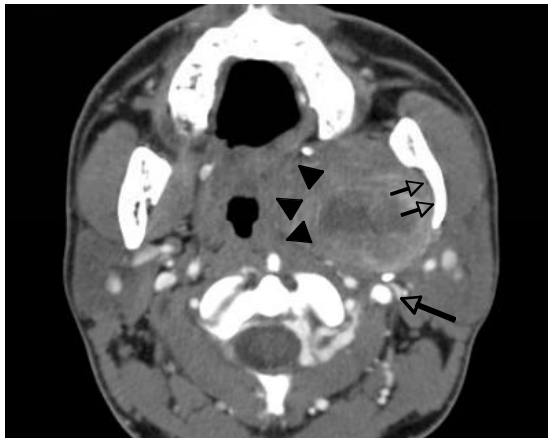

A

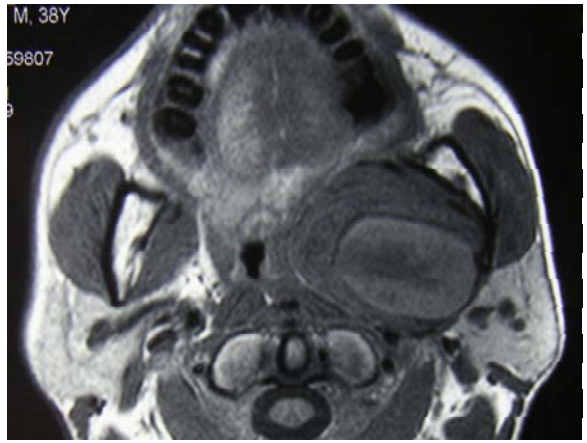

B

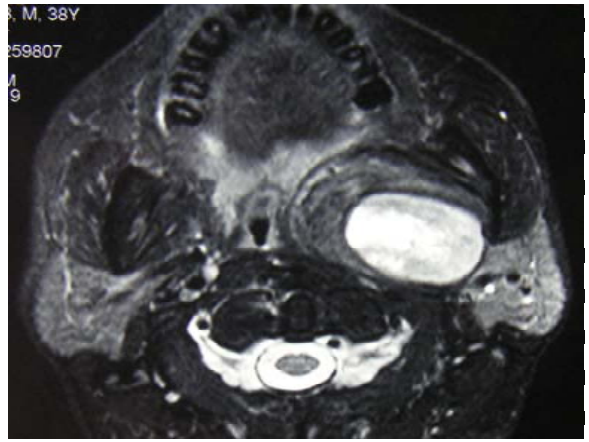

C

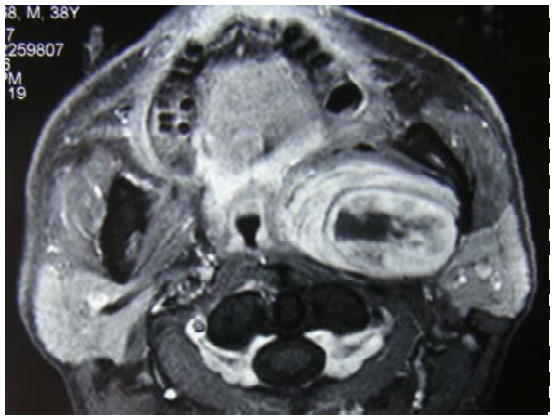

D

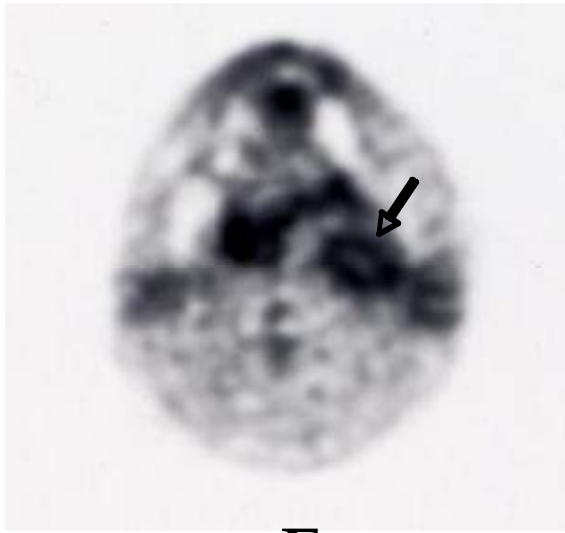

E

Fig. 1

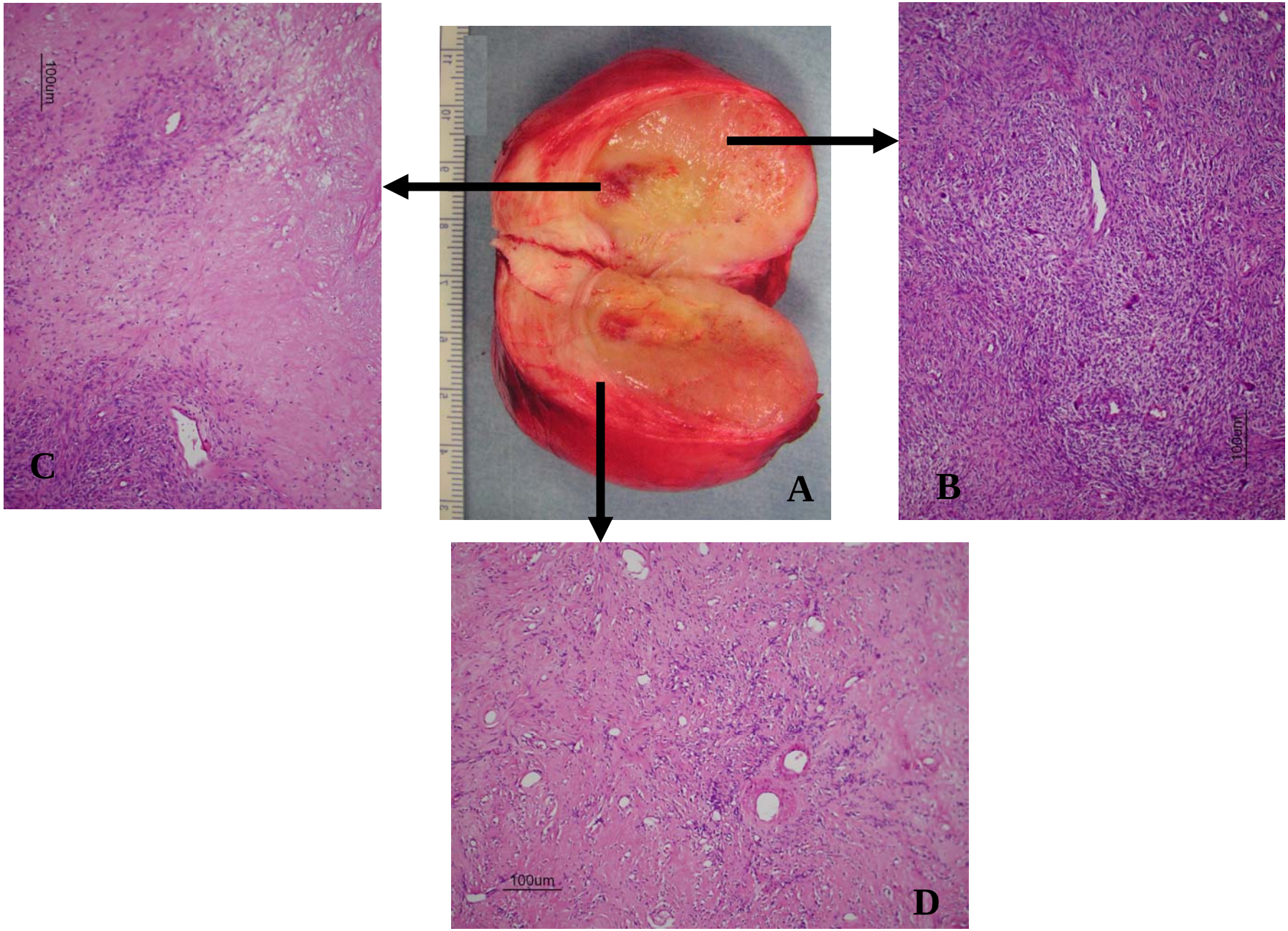

Fig. 2

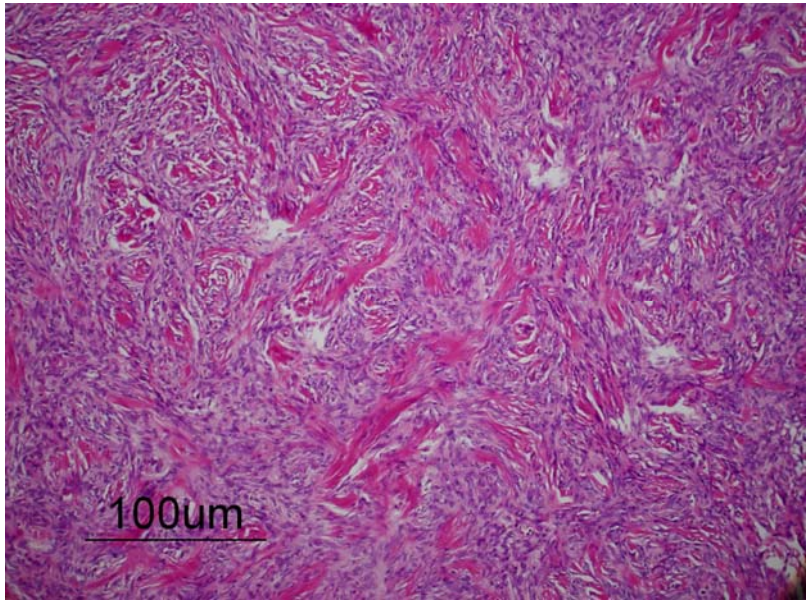

A

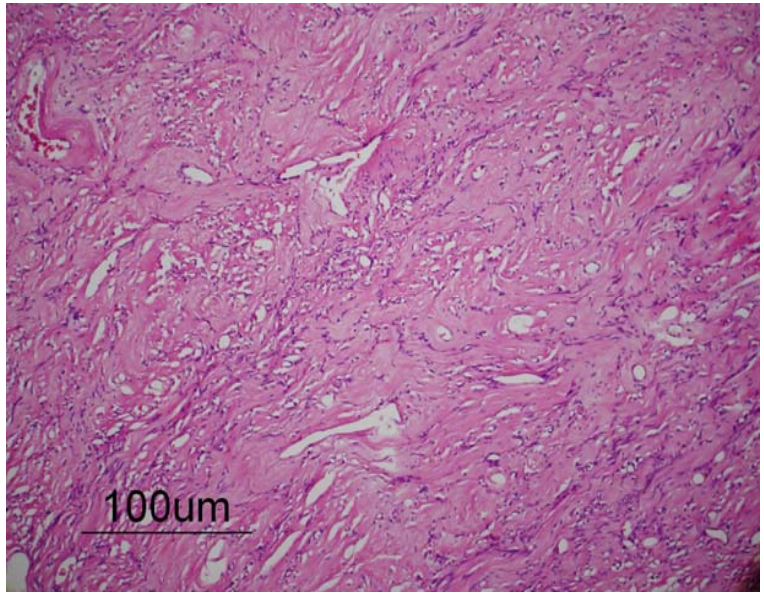

B

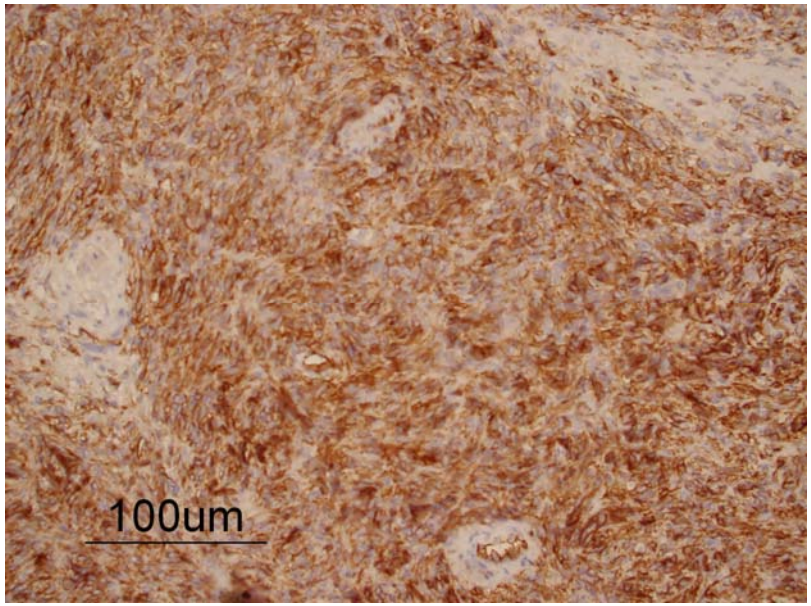

C

Fig. 3

Table: CT & MRI findings of solitary fabrous tumors arising in the parapharyngeal space

Author (Reference No.)	CT Findings	MRI Findings	FDG-PET Findings
Safneck, *et al* . (12)	heterogeneous enhanceme	ND	ND
Al-Sinawi, *et al* . (11)	ND	Gd-T１ : heterogeneous enhance	ND
Gangopadhyay, *et al* . (1	heterogeneous enhanceme	ND	ND
Sato, *et al* . (9)	heterogeneous enhanceme	T1: hypointensity T2: heterogeneous high intensity Gd-T１ : heterogeneous enhance	ND
Jeong, *et al* . (7)	ND	T1: isointensity T2: heterogeneous high intensity Gd-T1: homogeneous enhanceme	ND
Cizmarevic, *et al* . (6)	heterogeneous enhanceme	T2: heterogeneous high intensity	ND
Kim, *et al* . (3)	ND	T1: isointensity T2: heterogeneous high intensity Gd-T1: homogeneous enhanceme	ND
Hashimoto, *et al* . (5)	heterogeneous enhanceme	T1: homogeneous high intensity T2: heterogeneous high intensity	ND
Wakisaka, *et al* .	heterogeneous enhanceme	T1: hypo-isointensity T2: heterogeneous high intensity Gd-T1 : heterogeneous enhancem	heterogeneous uptake of FD

ND: not done; Gd: gadolinium-enhanced; FDG: ^{18}F-fluorodeoxyglucose.